Atmospheric Environment Vol. 25A, No. 11, pp. 2593–2606, 1991.
Printed in Great Britain.

0004–6981/91 $3.00+0.00

A THEORETICAL DETERMINATION OF THE COLLECTION RATES OF AEROSOL PARTICLES BY FALLING ICE CRYSTAL PLATES AND COLUMNS

N. L. MILLER
Environmental Research Division, Argonne National Laboratory, Argonne, IL 60439, U.S.A.

and

P. K. WANG
Department of Meteorology, University of Wisconsin, Madison, WI 53706, U.S.A.

(*First received* 28 *December* 1989 *and in final form* 10 *July* 1990)

Abstract—A theoretical model for the removal of aerosol particles by falling columnar ice crystals is compared to the model results for the removal of aerosol particles by falling planar ice crystals. These results incorporate gravitational, inertial, electrostatic, thermophoretic, diffusiophoretic, and Brownian diffusion mechanisms. Scavenging rates for columnar and planar ice crystals are computed for aerosol particles ranging from 0.001 to 10 μm in radius. The results show that planar ice crystals have greater collection efficiencies than the columnar ice crystals.

Key word index: Aerosol particles, collection rates, falling, ice crystals, scavenging model.

1. INTRODUCTION

Understanding the quantitative rates at which falling ice crystals scavenge the atmosphere of aerosol particles (APs) is a major concern. Until now, AP scavenging coefficients of falling ice crystals have been formulated as empirical values based on a few observations. This paper presents a theoretical model for accurate computation of AP scavenging coefficients of falling ice crystals as a function of gravity, inertia, electrostatic charge, thermophoresis, diffusiophoresis, and atmospheric variability.

Field investigations made by Carnuth (1967), Graedal and Franey (1975), and Magono *et al.* (1974, 1975) have indicated that falling ice crystals may remove APs up to 50 times more efficiently than does the equivalent liquid water content in falling raindrops. Field and laboratory studies have been unable to resolve detailed quantitative relationships among scavenging mechanisms and the atmosphere. Therefore, theoretical models verified by experimental and other theoretical results must be used.

Quantitative studies of scavenging mechanisms for aerosol particles of radii $0.001 \leqslant r \leqslant 10.0$ μm and their dependence on atmospheric variables were initiated by Greenfield (1957), who calculated raindrop–AP scavenging efficiencies. Since then many theoretical studies (e.g. Slinn and Hales, 1970, 1971; Pilat and Prem, 1976, 1977; Grover *et al.*, 1977; Wang *et al.*, 1978; Wang and Pruppacher, 1980a; Wang, 1983; Miller and Wang, 1989; Miller, 1990) and experimental studies (Beard and Grover, 1974; Wang and Pruppacher, 1977; Lai *et al.*, 1978; Leong *et al.*, 1982) have been carried out. Many of theoretical models produced results that agree closely with experimental values. The problem of drop–AP scavenging is therefore relatively well understood. In contrast, the scavenging of AP by ice crystals has not been as adequately studied.

Recently a few investigations have begun to theoretically evaluate ice scavenging (Wang and Pruppacher, 1980b; Martin *et al.*, 1980a, b; Wang 1985, 1989; Miller and Wang, 1989; Miller, 1987, 1990). The papers by Martin and coworkers dealt with planar ice crystals (PICs) and provided collection efficiencies for AP of radii 0.001–10.0 μm. Wang and Pruppacher (1980b) treated the scavenging of APs of radii 0.5 μm or less by columnar ice crystals (CICs). Their model and Wang's (1985, 1989) models are essentially flux models in which the effects of gravity and inertia are insignificant. Recent studies by Miller and Wang (1989) have provided collection efficiencies of falling CICs for APs with radii 0.001–10.0 μm. Miller (1987) has presented a theory for calculating the collection rates for APs with radii 0.001–10.0 μm of falling PICs and CICs, the two basic ice crystal shapes observed in the atmosphere. From the computed collection efficiencies, collection kernels and rates have been formulated.

2. MATHEMATICAL THEORY

The present theory extends the method of determining collection efficiencies to yield collection rates of

falling PICs and CICs for APs with radii 0.001–10.0 μm. The integrals of the products of the collection efficiencies with their respective geometric kernels and ice crystal size distributions will provide AP-size-dependent scavenging rates. Details of the theory of collection rates, collection kernels, and efficiencies and observed ice crystal size distributions are discussed in the following subsections.

2.1. *Aerosol particle collection rates*

Pruppacher and Klett (1978) defined the raindrop–AP collection rate, $\Lambda_r(r_p)$, which is dependent on AP radius r_p, as the integral of the product of the raindrop–AP collection kernel, $K_r(r_r, r_p)$, and the raindrop size distribution, $N_r(r_r)$, integrated with respect to raindrop radius, r_r,

$$\Lambda_r(r_p) = \int_0^\infty K_r(r_r, r_p) N_r(r_r)\, dr_r. \tag{1}$$

This definition lends itself to the calculation of ice crystal–AP collection rates

$$\Lambda_i(r_p) = \int_0^\infty K_i(r_i, r_p) N_i(r_i)\, dr_i, \tag{2}$$

where r_i, the ice crystal equivalent radius, is defined as the volume divided by the cross-sectional area perpendicular to the flow. $K_i(r_i, r_p)$ is the ice crystal collection kernel, and $N_i(r_i)$ is its size distribution. Ice crystal growth by diffusion occurs along perpendicular growth axes, and a cyclic plate–column–plate–column change in habit occurs due to temperature- and water vapor-dependent growth directions (Mason, 1971). Diffusionally grown ice crystals can be formulated as PICs and CICs so that these collection rates can be expressed as the sum of the PIC–AP collection rate, $\Lambda_{pl}(r_{pl}, r_p)$, and the CIC–AP collection rate, $\Lambda_c(r_c, r_p)$, as

$$\Lambda_i(r_p) = \Lambda_{pl}(r_p) + \Lambda_c(r_p), \tag{3}$$

where

$$\Lambda_{pl}(r_p) = \int_0^\infty K_{pl}(r_p) N_{pl}(r_{pl})\, dr_{pl} \tag{4a}$$

and

$$\Lambda_c(r_p) = \int_0^\infty K_c(r_c, r_p) N_c(r_c)\, dr_c. \tag{4b}$$

The composite scavenging rate $\Lambda_i(r_p)$ represents only simple, diffusionally grown ice crystals and does not apply to all ice crystal shapes. The PIC collection kernel, $K_{pl}(r_{pl}, r_p)$, is dependent on PIC and AP equivalent radii, the CIC collection kernel, $K_c(r_c, r_p)$, is dependent on CIC and AP equivalent radii; and $N_{pl}(r_{pl})$ and $N_c(r_c)$ are the PIC and CIC size distributions.

2.2. *Aerosol particle collection kernels*

Collection kernels for both ice crystal types are based on complementary models that indicate collection efficiencies for APs of radii 0.001–10.0 μm. These models are: (1) a trajectory model for APs 0.5 μm and larger and (2) a flux model for APs 0.5 μm and smaller. The product of the collection efficiency and its respective geometric kernel defines the collection kernel as

$$K_{pl}(r_{pl}, r_p) = E_{pl}(r_{pl}, r_p) K^*_{pl}(r_{pl}, r_p) \tag{5a}$$

and

$$K_c(r_c, r_p) = E_c(r_c, r^*_p) K_c(r_c, r_p), \tag{5b}$$

where $E_{pl}(r_{pl}, r_p)$ and $E_c(r_c, r_p)$ are the collection efficiencies for PICs and CICs, respectively. Efficiencies are discussed in sections 2.3 and 2.4. The geometric kernel is defined as the total volume swept out per unit time by an ice crystal with cross-sectional area equal to the sum of the radii of the ice crystal and the AP, falling at the terminal velocity of the ice crystal relative to the AP, as

$$K^*_{pl}(r_{pl}, r_p) = \pi(r_{pl} + r_p)^2 (V_{pl} - V_p) \tag{6a}$$

and

$$K^*_c(r_c, r_p) = (r_c + 2r_p)(l_c + 2r_p)(V_c - V_p), \tag{6b}$$

where V_{pl}, V_c, and V_p are the terminal fall velocities of PICs, CICs, and APs, respectively, and l_c is the CIC length.

2.3. *The trajectory model*

Collection efficiency particle trajectory models are based on Newton's second law of motion. The AP position relative to a falling ice crystal, $\mathbf{R}(t)$, is a time-integrated function from the equation of motion

$$\frac{d^2\mathbf{R}(t)}{dt^2} = \frac{1}{m_p}[\mathbf{F}_g + \mathbf{F}_d + \mathbf{F}_e + \mathbf{F}_{th} + \mathbf{F}_{df}], \tag{7}$$

where m_p is the AP mass; $\mathbf{F}_g$ is the buoyancy-corrected gravitational force,

$$\mathbf{F}_g = \mathbf{g}(\rho_p - \rho_a)/\rho_p, \tag{8}$$

$\mathbf{g}$ is the gravitational acceleration; ρ_p is the bulk density of the particle; and ρ_a is the air density.

The drag force, $\mathbf{F}_d$, is due to air mass resistance, which is proportional to the difference in velocities between the AP [$\mathbf{v}_p = d\mathbf{R}(t)/dt$] and the incompressible flow of air across the PIC or CIC, where $\mathbf{u}$ is determined by solving the full Navier–Stokes equations for each PIC and CIC.

The drag force on an assumed spherical particle is expressed as

$$\mathbf{F}_d = -6\pi\eta_a r_p(\mathbf{v}_p - \mathbf{u})/C_{sc}. \tag{9}$$

This Stokes drag force has a dynamic air viscosity η_a. The Stokes–Cunningham slip correction factor has been defined as $C_{sc} = 1.0 + \alpha N_{Kn}$, where $\alpha = 1.26 + 0.40\exp(-1.1/N_{Kn})$. The Knudsen number, $N_{Kn} = \lambda/r_p$, is the ratio of the free path length of molecules in air, λ, to the particle radius, r_p.

The electrostatic force, $\mathbf{F}_e$, on a particle near a charged ice crystal is

$$\mathbf{F}_e = -Q_p \nabla \phi_e. \tag{10}$$

As in the model of Wang *et al.* (1978), the particle point charge is represented as $Q_p = qr_p^2$, where the constant q ranges from 0.2 to 2.0 esu cm^{-2}, the mean charge values for hydrometeors in thunderstorms. The electric potential, ϕ_e, has been defined by Martin *et al.* (1980a) for PICs and by Miller and Wang (1989) for CICs.

Thermophoretic forcing, $\mathbf{F}_{th}$, occurs in nonsaturated air, with respect to water vapor, and was given by Brock (1962) as

$$\mathbf{F}_{th} = C_{th} \nabla T \tag{11}$$

where

$$C_{th} = -12\pi\eta_a r_p (k_a + 2.5 k_p N_{Kn})/ [5(1+3N_{Kn})(k_p + 2k_a + 5k_p N_{Kn}) P], \tag{12}$$

k_a is the thermal conductivity of air, k_p is the thermal conductivity of the particle, and P is the atmospheric pressure.

The diffusiophoretic force, $\mathbf{F}_{df}$, also occurs in nonsaturated air. The diffusiophoretic force is given as (Hidy and Brock, 1970)

$$\mathbf{F}_{df} = C_{df} \nabla \rho_v, \tag{13}$$

where

$$C_{df} = -6\pi\eta_a r_p (0.74 D_{va} M_a)/[(1+\alpha N_{Kn}) M_w \rho_a]. \tag{14}$$

In this study, the diffusivity of water vapor in air, D_{va}, is assumed constant for each specified ambient temperature and pressure. The molecular weights of dry air and water are M_a and M_w, respectively.

The temperature and water vapor density fields are computed as the solutions to the temperature and vapor density convective–diffusion equations for each PIC (Martin *et al.*, 1980a) and CIC (Miller and Wang, 1989).

Collision efficiencies of APs greater than 0.5 μm are determined by the trajectory model, with the assumption that the particle fields do not affect the ice crystal velocity, water vapor, and temperature fields (Martin *et al.*, 1980a; Miller and Wang, 1989). This assumption is justified by requiring that r_p/r_{pl} and r_p/r_c be less than 0.5 (Grover, 1980). The collision efficiency of PICs in the trajectory model is given as (Martin *et al.*, 1980a)

$$E_{pl}(r_{pl}, r_p) = y_c^2/(r_{pl} + r_p)^2. \tag{15}$$

The collision efficiency of CICs in the trajectory model is defined as (Miller and Wang, 1989)

$$E_c(r_c, r_p) = y_c/(r_c + r_p), \tag{16}$$

where y_c is the maximum initial horizontal offset from an axis perpendicular to the PIC or CIC (with the positive x-direction parallel to the Earth's gravity) and in the free stream that yields a trajectory just grazing the crystal.

2.4. *The flux model*

An analytical flux model to determine collection efficiencies for the convective diffusion of APs with radii less than 0.5 μm for either PICs or CICs was formulated by Wang (1985). This model considers Brownian diffusion and electrostatic, thermophoretic, and diffusiophoretic forcing. Effects due to gravity are negligible in this size range. The flux density of APs toward an ice crystal is given as

$$\mathbf{j}_p = n\mathbf{V}_{\text{drift}} - \bar{f}_p D_B \nabla n, \tag{17}$$

where n is the particle concentration. The drift velocity is defined as

$$\mathbf{v}_{\text{drift}} = B(\mathbf{F}_e + \bar{f}_h \mathbf{F}_{th} + \bar{f}_v \mathbf{F}_{df}). \tag{18}$$

The mobility is defined as $B = C_{sc}/(6\pi\eta_a r_p)$ and the Brownian diffusion coefficient as $D_B = BkT$, k is the Boltzman constant, and T is the air temperature. The Brownian, thermal, and vapor ventilation factors, $\bar{f}_p$, $\bar{f}_h$, and $\bar{f}_v$, are calculated by using the empirical formulas of Hall and Pruppacher (1976). Steady-state conditions result in the conservation of particle concentration, $\nabla \cdot \mathbf{j}_p = 0$. Assuming that the forces are nondivergent and conservative will lead to the steady-state-ventilation-enhanced, convective–diffusion equation.

$$\mathbf{v}_{\text{drift}} \cdot \nabla n - \bar{f}_p D_B \nabla^2 n = 0. \tag{19}$$

A force potential, ϕ_f, is defined such that $\nabla^2 \phi_f = 0$ and $\nabla \phi_f = -(\mathbf{F}_e + \bar{f}_h \mathbf{F}_{th} + \bar{f}_v \mathbf{F}_{df})$. The solution to Equation (19) satisfying the boundary conditions $n = 0$ at the ice crystal surface and $n = n_\infty$ at the free stream was given by (Wang, 1985, 1989) as

$$n = \frac{n_\infty \{\exp[B(\phi_{f,s} - \phi_f)/DB] - 1\}}{\exp(B\phi_{f,s}/D_B) - 1}, \tag{20}$$

where

$$\phi_{f,s} = Q_p/C_c + C_{th}(T_\infty - T_s) + C_{df}(\rho_{v,s} - \rho_{v,s}) \tag{21}$$

is the total force potential at the surface of PICs or CICs and C_c is the respective capacitance. The resulting collision kernel for a particle flux is

$$K_i(r_i, r_p) = -(1/n_\infty)\frac{\partial}{\partial t}\int_{r_p}^{\infty} n(r_p)\, dr_p \tag{22a}$$

$$= -4\pi B \phi_{f,s} C_c/[\exp(B\phi_{f,s}/D_B) - 1]. \tag{22b}$$

The PIC and CIC collection efficiencies are defined as the ratios of the collection kernels to their respective geometric kernels,

$$E_{pl}(r_{pl}, r_p) = K_i(r_{pl}, r_p)/K_{pl}^*(r_{pl}, r_p) \tag{23a}$$

and

$$E_c(r_c, r_p) = K_i(r_c, r_p)/K_c^*(r_c, r_p). \tag{23b}$$

Collection efficiencies are equivalent to collision efficiencies if no rebound of particles is assumed to occur from the ice crystal surface after a collision.

3. ICE CRYSTAL SIZE DISTRIBUTION

The normalized size distributions for ice crystals used in this study are based on ground observations measured simultaneously at three sites in the Cascade Mountains of Washington state during orographic precipitation events in the 1971–1972 snow season (Hobbs *et al.*, 1972). Figure 1 shows the size distributions. Figure 2 shows a histogram of the frequency of occurrence of the various types of snow particles. These results indicate that columnar ice crystals and graupel occur most frequently, followed by dendrites, graupel snow, needles, plates, stellars, and bullets. The size distributions are normalized about their maximum value,

$$N_{i,n}(r_i) = N_i(r_i)/N_{i,\max}(r_{i,m}), \tag{24}$$

where i ranges from 1 to 13 and represents the crystal types shown in Fig. 2, and the subscript n indicates normalization. This normalization removes from the model the absolute amount of ice particles but maintains the overall size-dependent distribution. Normalizing ice crystal size distributions will allow additional ice crystal distributions to be used later. Integrating Equations (4a and b) with normalized size distributions will produce normalized collection rates by PICs and CICs. These normalized collection rates are used here to quantitatively determine rates of AP removal by falling ice crystals as a function of AP size.

When the normalized collection rates are multiplied (scaled) by observed $N_{c,\max}$ or $N_{pl,\max}$ values, the absolute AP-size-dependent collection rates are determined.

4. METHODS OF EVALUATION

The computed results presented here correspond to an atmospheric pressure of 600 mb and an ambient temperature of -20°C unless otherwise noted. Values for $\rho_a(T)$ are from the Smithsonian Meteorological Tables. Values of $k_a(T)=(5.69+0.017\,T°\text{C})\times10^{-5}$; $k_p(T)=(3.78+0.020\,T°\text{C})\times10^{-5}$; $\lambda(P,T)=6.6\times10^{-6}$ cm $(1013.25\text{ mb/P})(T/293.15\text{ K})$; $D_{va}(P,T)=0.211(T/273.15\text{ K})^{1.94}(1013.25\text{ mb/P})$; and $\eta_a(T)=(1.718+0.0049T-1.2\times10^{-5}\,T^2)\times10^{-4}$, $T(°\text{C})<0$, are from Pruppacher and Klett (1978). The bulk densities for the ice crystals and the aerosol particles are 0.6 and 2.0 g cm^{-3}, respectively, unless otherwise noted.

5. RESULTS AND DISCUSSION

Figures 3a–g indicate computed values of collection kernels as a function of AP size for the set of seven CICs ($0.5\leqslant N_{Re}\leqslant20.0$) at (1) 95%, (2) 75%, and (3) 50% relative humidity (r.h.), with and without electric

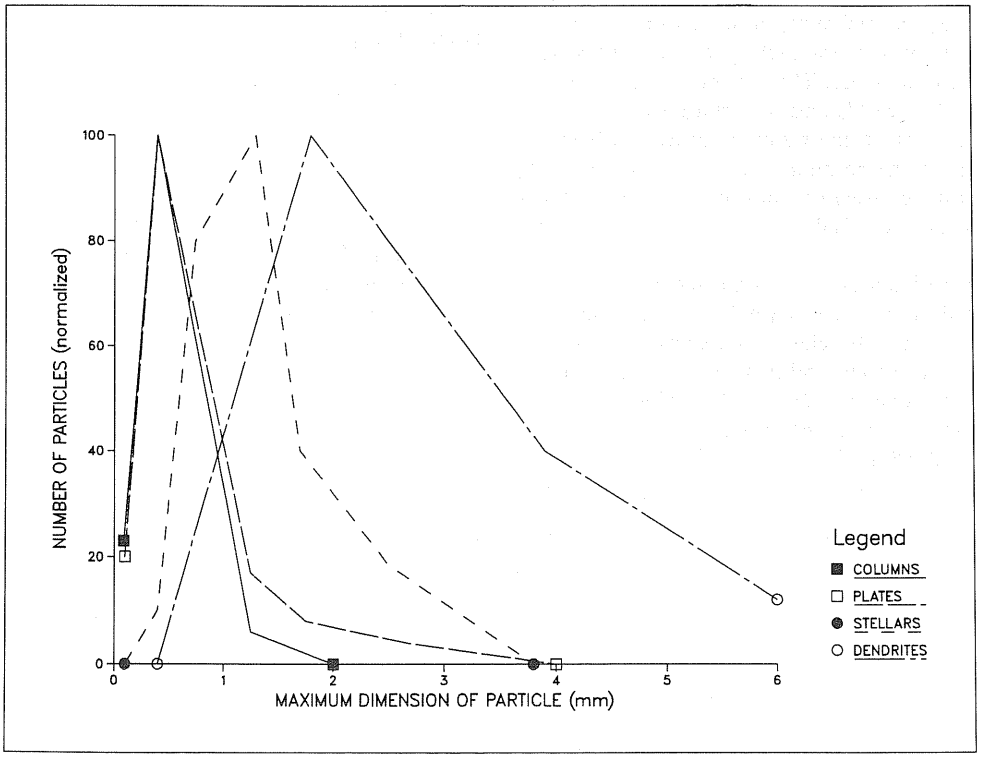

Fig. 1. Size distribution of snow crystals collected at Alpental Base, Hyak, and Keechelus Dam, Washington (from Hobbs *et al.*, 1972).

charge (e). This range corresponds to columnar ice crystal lengths of $93 \leqslant l_c \leqslant 2440$ μm and is representative of the CIC size spectrum in the ice particle distributions of Fig. 1. The shapes of these kernels are very similar to the collection efficiency curves of Miller and Wang (1989). However, the collection kernel increases with increasing N_{Re}, whereas collection efficiencies decrease with increasing N_{Re}. This difference is due to the geometric kernel's dependence on the CIC's terminal velocity and cross-sectional area perpendicular to the flow. While the collection efficiency decreases, the collection kernel and hence the absolute number of APs scavenged increase with increasing CIC size. The CIC collection kernels exhibit a more flattened behavior across the region $0.01 \leqslant r_p \leqslant 1.0$ μm than the efficiency curves. An observed zero collection zone (ZCZ) for collection kernels is located in the same AP position as for the collection efficiency values (Miller and Wang, 1989; Miller, 1987; Grover *et al.*, 1977).

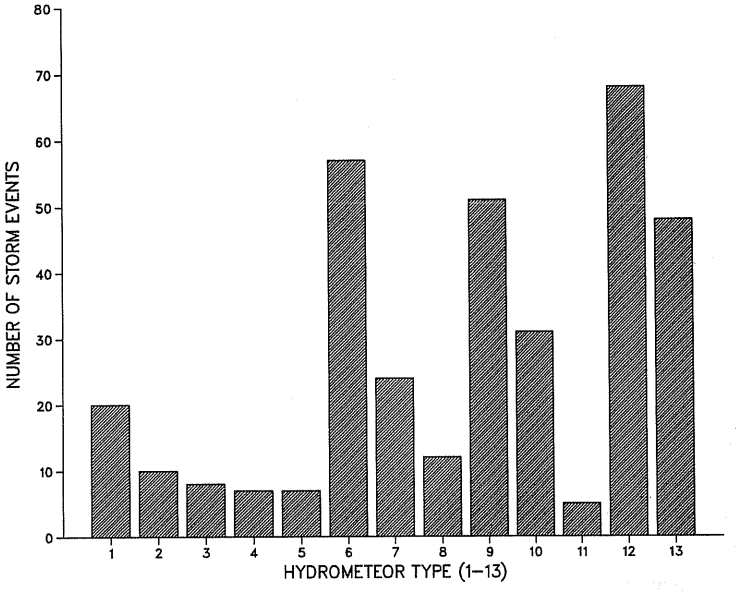

Fig. 2. Histogram of the relative frequencies of occurrence of (1) ice crystal plates, (2) bullets, (3) side planes, (4) assemblages of sectors, (5) assemblages of plates, (6) columnar ice crystals, (7) needles, (8) stellars, (9) dendrites, (10) radiating assemblages of plates, (11) crystals with broad branches, (12) graupel, and (13) graupel snow measured at Alpental Base (from Hobbs *et al.*, 1972).

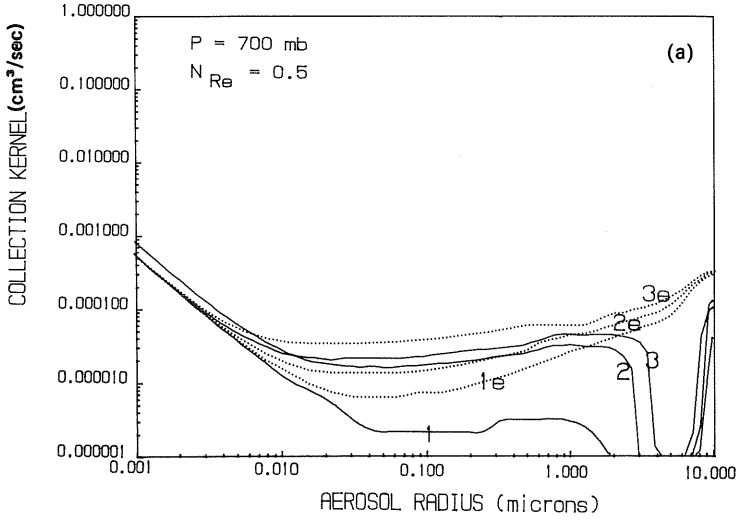

Fig. 3a.

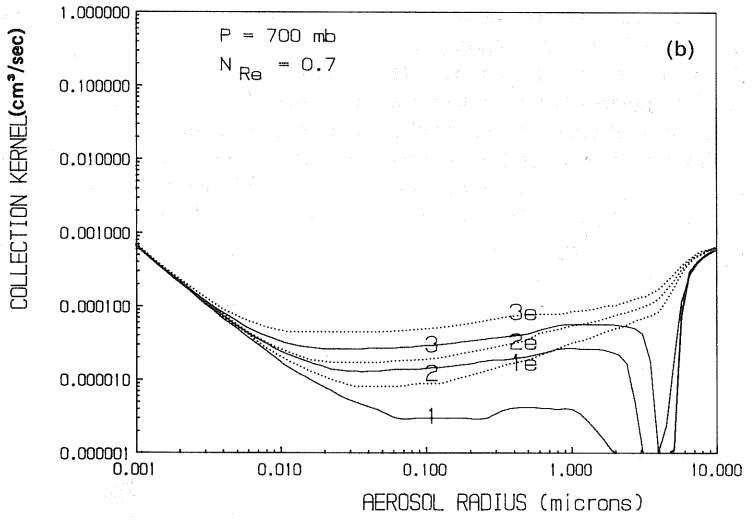
P = 700 mb
N Re = 0.7
(b)
COLLECTION KERNEL(cm³/sec)
1.000000
0.100000
0.010000
0.001000
0.000100
0.000010
0.000001
0.001
0.010
0.100
1.000
10.000
AEROSOL RADIUS (microns)
3e
3
2e
2
1e
1

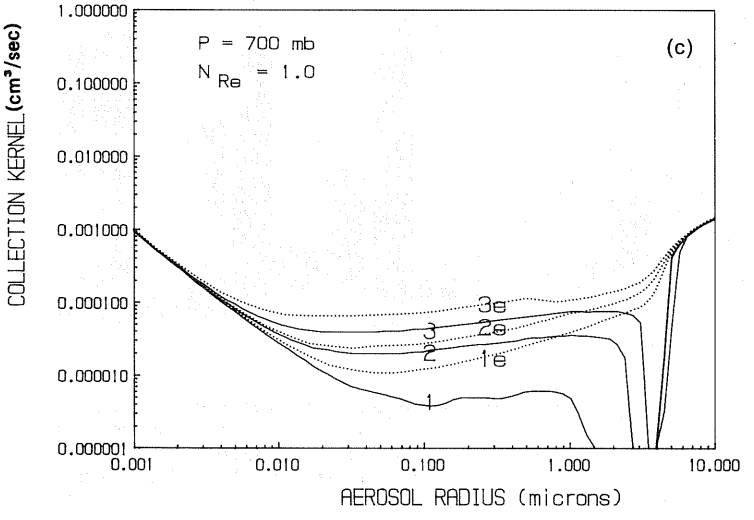
P = 700 mb
N Re = 1.0
(c)
COLLECTION KERNEL (cm³/sec)
1.000000
0.100000
0.010000
0.001000
0.000100
0.000010
0.000001
0.001
0.010
0.100
1.000
10.000
AEROSOL RADIUS (microns)
3e
3
2e
2
1e
1

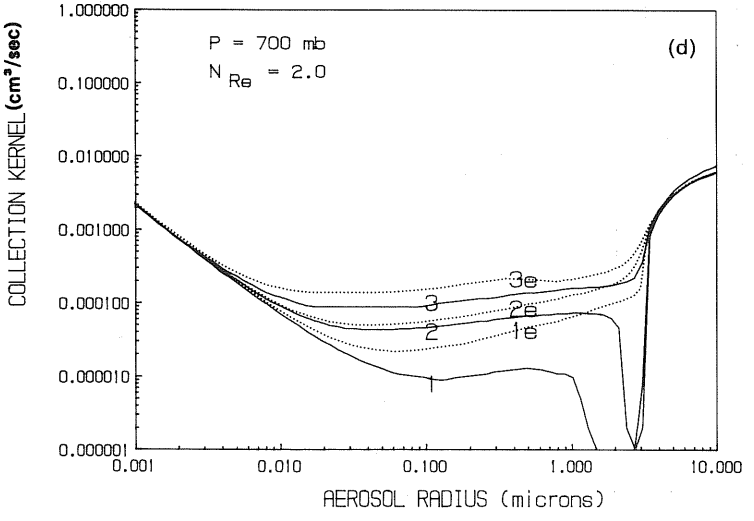
P = 700 mb
N Re = 2.0
(d)
COLLECTION KERNEL (cm³/sec)
1.000000
0.100000
0.010000
0.001000
0.000100
0.000010
0.000001
0.001
0.010
0.100
1.000
10.000
AEROSOL RADIUS (microns)
3e
3
2e
2
1e
1

Fig. 3b–d.

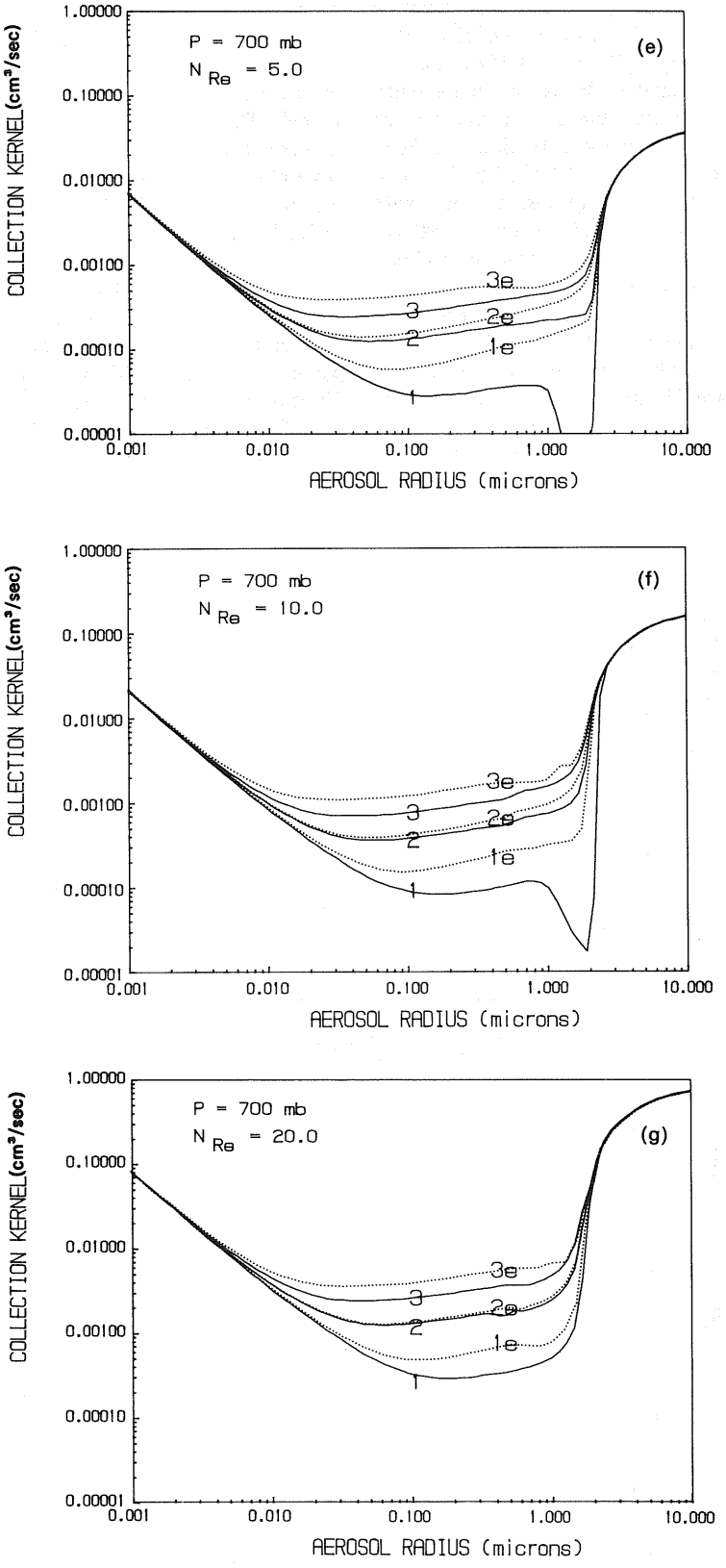

Fig. 3. Collection kernels by columnar ice crystals at 700 mb and 263 K with (1) 95%, (2) 75%, and (3) 50% r.h. and with electrostatic charge (*e*) $q=2$ esu cm^{-2} for (a) $N_{Re}=0.5$, (b) $N_{Re}=0.7$, (c) $N_{Re}=1.0$, (d) $N_{Re}=2.0$, (e) $N_{Re}=5.0$, (f) $N_{Re}=10.0$, and (g) $N_{Re}=20.0$.

Figures 4a–h indicate computed values of collection kernels as a function of AP size for a set of eight PICs ($0.1 \leqslant N_{Re} \leqslant 50.0$) at (1) 95% and (2) 50% r.h. The values are based on available PIC–AP collection efficiency data (Martin *et al.*, 1980a, b). These discrete collection kernels represent the collection of APs of radius $0.001 \leqslant r_p \leqslant 2.0$ μm by PICs with $0.1 \leqslant N_{Re} \leqslant 50.0$. This wide N_{Re} range represents PICs with characteristic lengths (plate diameters) of $90 \leqslant l_{pl} \leqslant 1112$ μm, which is a slightly smaller ice crystal size range than for CICs but represents over 95% of all PICs. There are indications of a ZCZ in Figs 4c–e. Unfortunately, the available PIC–AP data do not extend beyond 2 μm, where the collection efficiencies presumably increase. The apparent ZCZ occurs in the same AP size region (i.e. it is centered at approximately 2 μm) as the ZCZs observed in the CIC–AP model. A ZCZ also occurs at about 2 μm in the drop–AP collection efficiency model of Wang *et al.* (1978).

PICs have greater collection efficiencies than CICs of the same N_{Re} because of their larger geometric kernels. The PIC geometric kernels have a larger, flat ice surface perpendicular to the flow, which causes the streamlines to diverge and form eddies at much lower N_{Re} than for CICs. The divergent streamline pattern hydrodynamically forces APs to spend a longer time near the PIC collector surface than near a CIC collector surface. The fact that PICs form eddies at lower N_{Re} than do CICs implies that more eddy-induced back capture occurs for PICs. Figure 5 compares CIC–AP and PIC–AP collection efficiencies at 700 mb and 95% r.h. for four AP sizes, (1) 0.001, (2) 0.01, (3) 0.1, and (4) 1.0 μm, as a function of equivalent ice crystal geometric kernels. This figure shows that

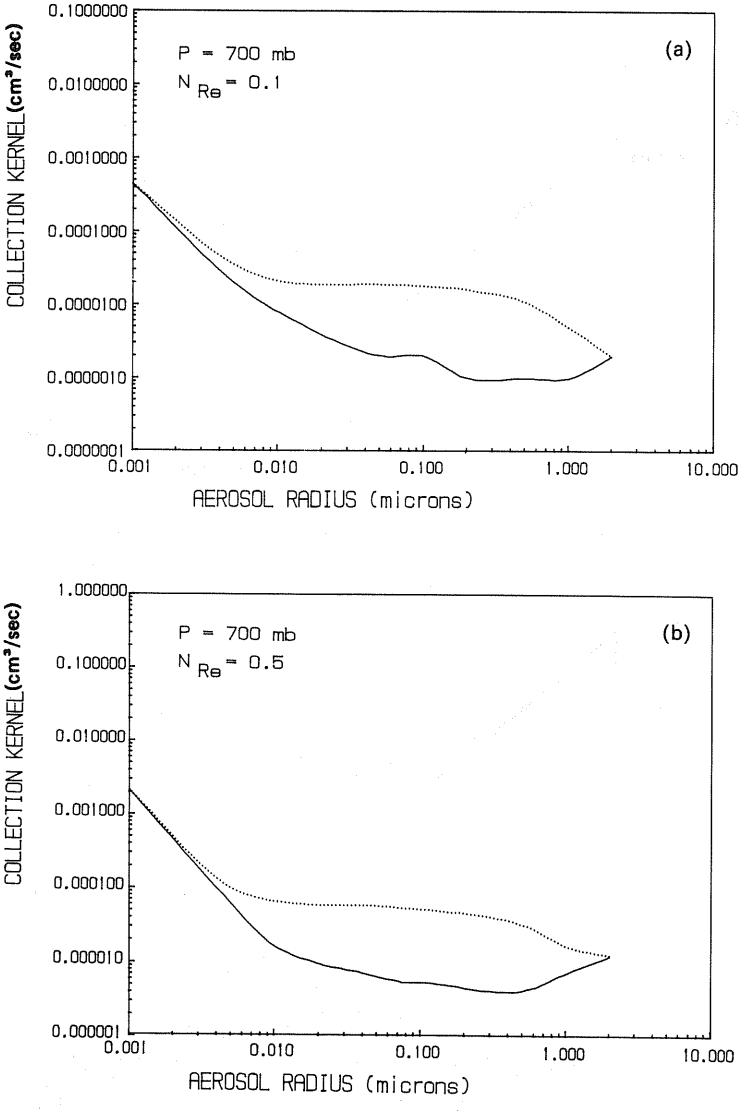

Fig. 4a–b.

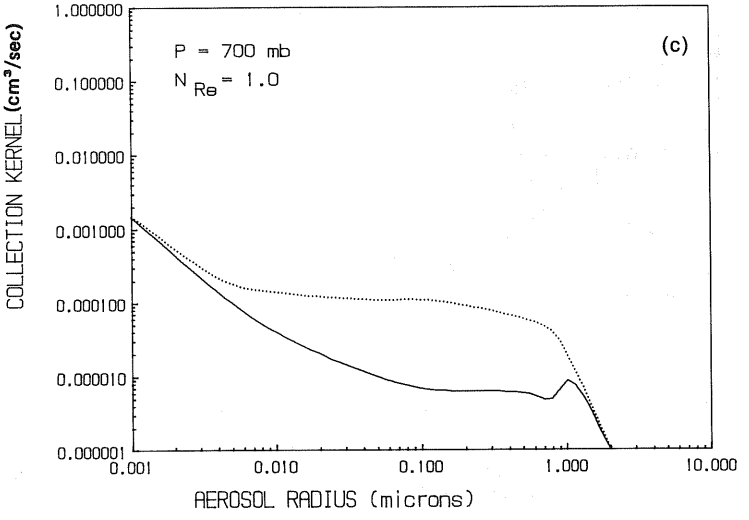
1.000000
0.100000
0.010000
0.001000
0.000100
0.000010
0.000001
COLLECTION KERNEL (cm³/sec)
P = 700 mb
N Re = 1.0
(c)
0.001
0.010
0.100
1.000
10.000
AEROSOL RADIUS (microns)

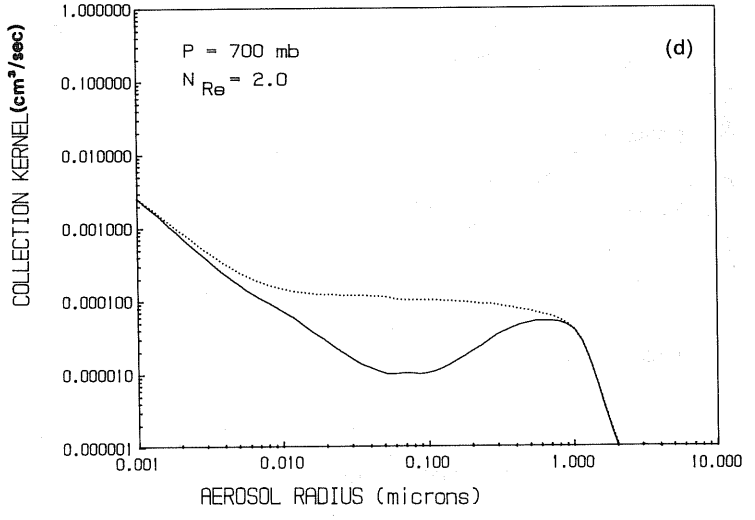
1.000000
0.100000
0.010000
0.001000
0.000100
0.000010
0.000001
COLLECTION KERNEL (cm³/sec)
P = 700 mb
N Re = 2.0
(d)
0.001
0.010
0.100
1.000
10.000
AEROSOL RADIUS (microns)

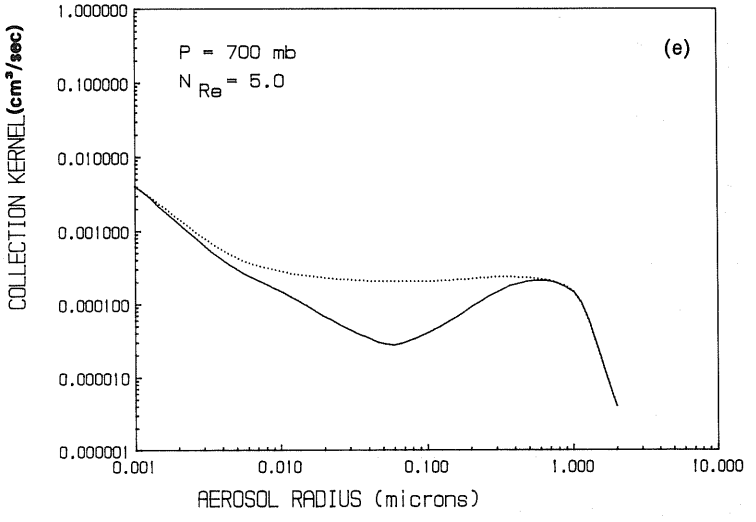
1.000000
0.100000
0.010000
0.001000
0.000100
0.000010
0.000001
COLLECTION KERNEL (cm³/sec)
P = 700 mb
N Re = 5.0
(e)
0.001
0.010
0.100
1.000
10.000
AEROSOL RADIUS (microns)

Fig. 4c–e.

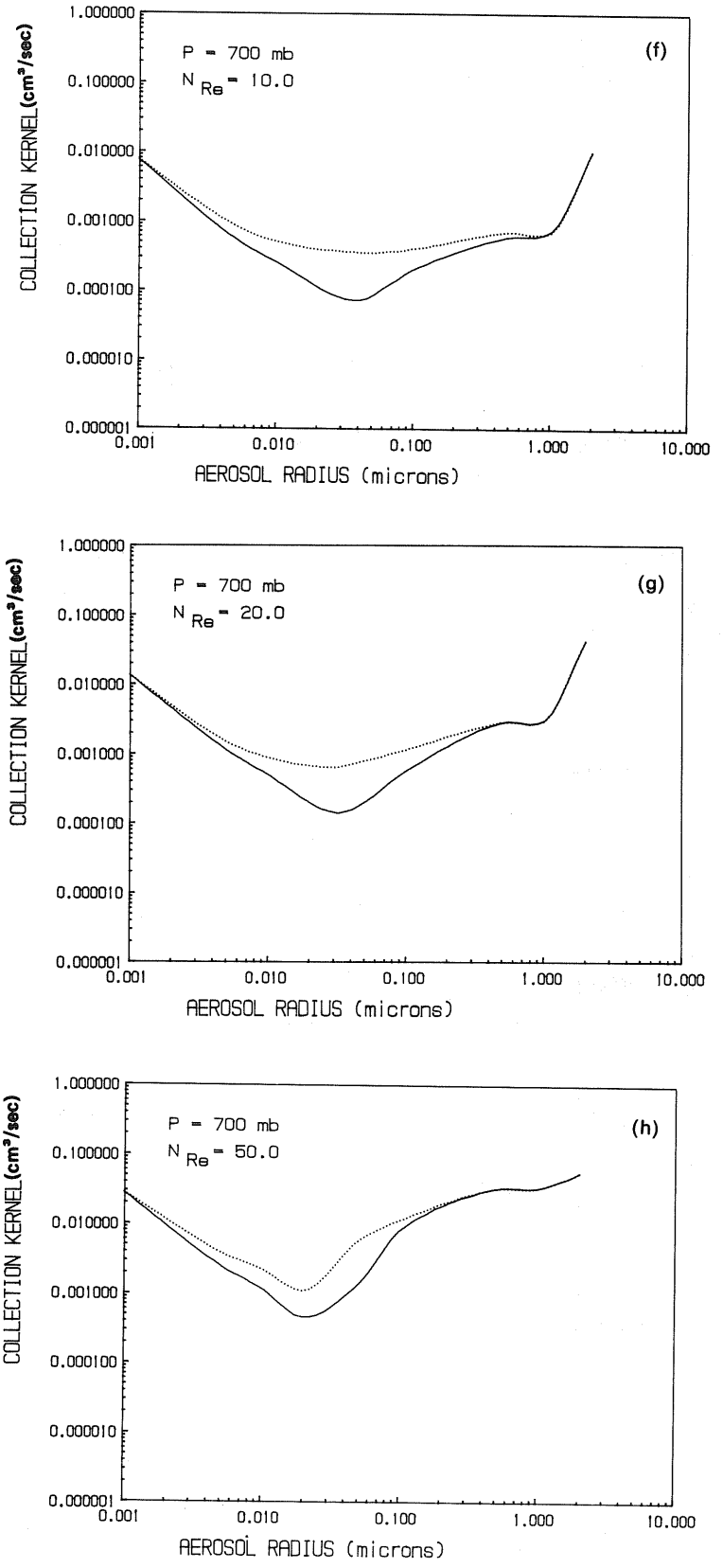

Fig. 4. Collection kernels by columnar ice crystal plates at 700 mb and 263 K with (1) 95% and (2) 50% r.h. for (a) $N_{Re}=0.1$, (b) $N_{Re}=0.5$, (c) $N_{Re}=1.0$, (d) $N_{Re}=2.0$, (e) N_{Re}, (f) $N_{Re}=10.0$, (g) $N_{Re}=20.0$, and (h) $N_{Re}=50.0$.

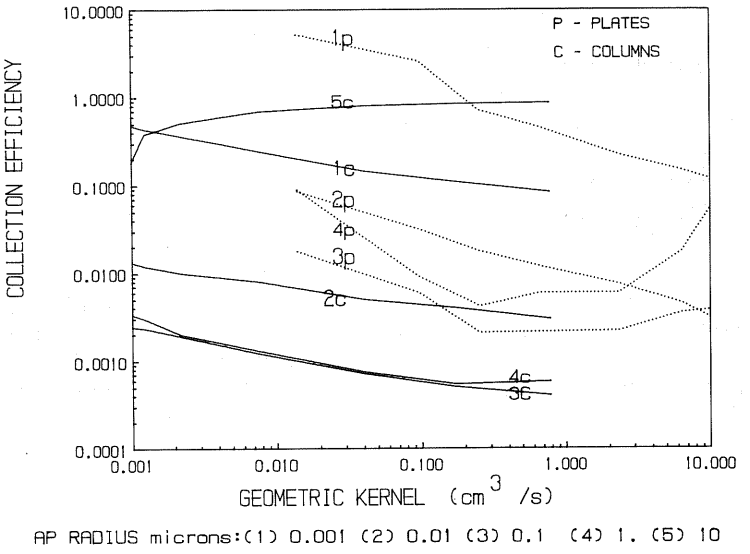

Fig. 5. Collection efficiency as a function of geometric kernel for APs of radii (1) 0.001, (2) 0.01, (3) 0.1, (4) 1.0, and (5) 10.0 μm by (*c*) columnar ice crystals and (*p*) ice crystal plates at 700 mb, with 95% r.h.

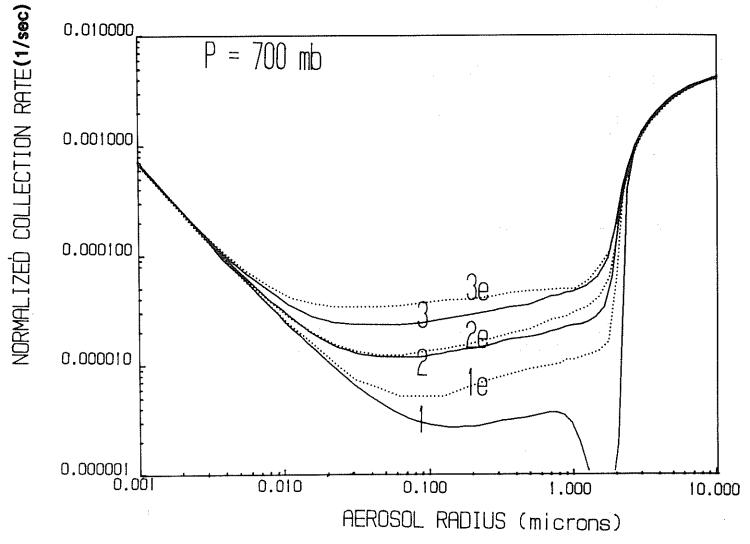

Fig. 6. Normalized collection rates for APs of columnar ice crystals at 700 mb and 263 K. Curves are for r.h. of (1) 95%, (2) 75%, and (3) 50% with and without electrostatic charge (*e*) $q=2$ esu cm^{-2}.

PICs are better AP collectors than CICs across the AP size range 0.1–2.0 μm. The PIC–AP collection kernels with $N_{Re}>2$ have a well-defined collection minimum in the $0.2<r_p<0.7$ μm region. This finding is in agreement with the CIC–AP model and the Wang *et al.* (1978) drop–AP model.

The numerical integration for computing the normalized PIC and CIC collection rates, $\Lambda_{pl,n}(r_p)$ and $\Lambda_{c,n}(r_p)$, uses the trapezoid method. A more elaborate integration technique would not decrease the error of the total calculation. Figure 6 shows computed normalized columnar ice crystal collection rates at 700 mb, 263 K, and (1) 95%, (2) 75%, and (3) 50% r.h. with and without electric charge (*e*). This level was chosen to match the data provided by Hobbs *et al.* (1972) and to use the PIC collection efficiencies of Martin *et al.* (1980a, b).

Each curve in Fig. 6 has characteristics representative of its respective kernel. The phoretic effect is maximized near 1.0 μm, and the electrostatic effect maintains a collection enhancement similar to that seen in Figs 3a–g. A ZCZ exists for APs with

$1.0 \leqslant r_p \leqslant 2.0$ μm at r.h. above 95%. Most important is the evidence that the collection rates are insensitive to small differences in ice crystal distributions. Only the peak values for ice crystals will affect the collection rate if the ice crystal size distribution function remains constant. Therefore, the maximum values $N_{c,\max}$ and $N_{pl,\max}$, not the distribution, are of concern.

Normalized collection rates are converted into absolute collection rates by multiplying each value by an observed maximum number of CICs or PICs per size interval, dr_c. Figure 7 indicates that the absolute collection rates are identical to the normalized values except for a shift in the collection rate scale. This illustrates the linearity between the absolute and normalized collection rates.

The PIC collection rates were computed similarly to the CIC collection rates. PIC distributions are of the same general shape as CIC distributions, but they have a different $N_{\max}$ and overall size range. The computed PIC collection rates are plotted in Fig. 8 along with the corresponding collection rates for CICs for an atmosphere at 700 mb and 263 K for (1) 95% and (2) 50% r.h. The collection rates for PICs and CICs converge in the region where Brownian diffusion is the dominant collection mechanism. This solution reinforces Wang's (1985) diffusion model, which calculates Brownian diffusion independently of the collector geometry. Beyond $r_p \simeq 0.02$ μm, PICs show significantly greater collection rates with an order of magnitude difference near $r_p = 1.0$ μm. PICs have a min-

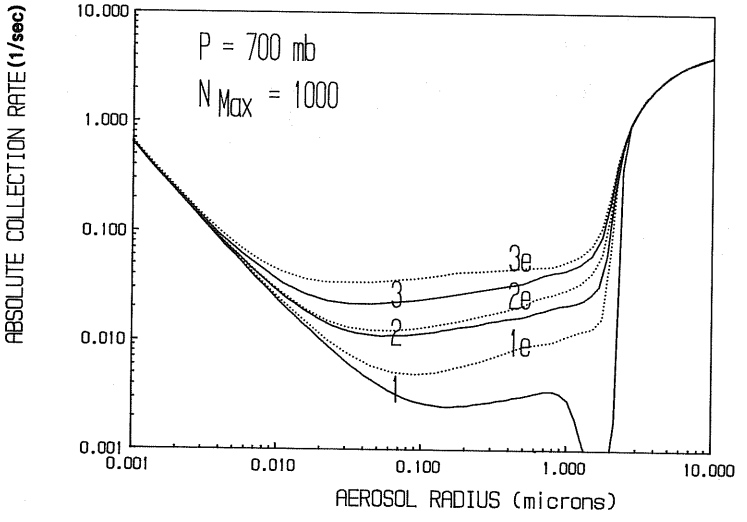

Fig. 7. Absolute collection rates for APs of columnar ice crystals at 700 mb and 263 K, with $N_{\max} = 1000$. Curves are for r.h. values of (1) 95%, (2) 75%, and (3) 50%, with and without electrostatic charge (e) $q = 2$ esu cm^{-2}.

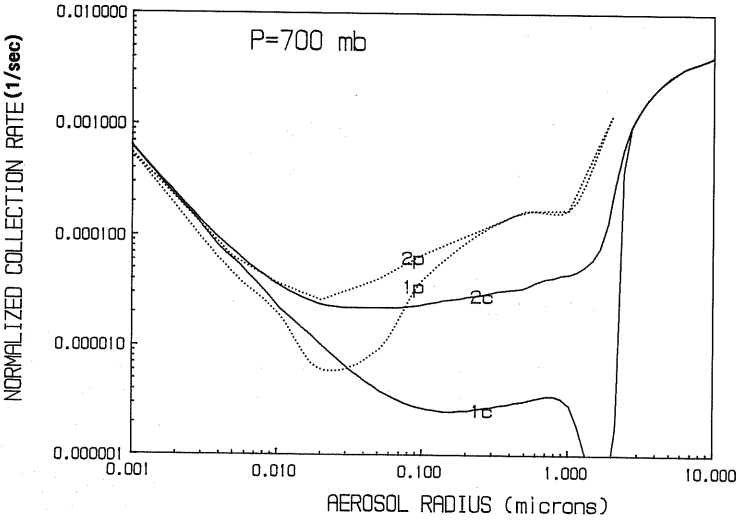

Fig. 8. Normalized collection rates for APs of columnar ice crystals (C) and ice crystal plates (P). Curves for r.h. of values (1) 95% and (2) 50% are shown.

imum collection rate at about 0.01 μm, while CICs have a minimum near 0.3 μm. These differences are due in part to the large flat surfaces of plates. These results confirm that plates are more efficient collectors than columns under the studied sets of conditions. These results can be extended to atmospheric conditions and ice crystal distributions to provide a complete ice crystal collection scheme.

Absolute collection rates are obtained by multiplying the normalized collection rates by their respective maximum ice crystal size distribution values,

$$\Lambda_{pl,abs}(r_p) = \Lambda_{pl,n}(r_p) N_{\max}(r_{pl,\max}) \quad (25a)$$

and

$$\Lambda_{c,abs}(r_p) = \Lambda_{c,n}(r_p) N_{\max}(r_{c,\max}). \quad (25b)$$

The results from Equations (25a and b) can be inserted into Equation (3) to accurately yield ice crystal–AP collection rates. The fact that the shape of the curve for Λ is essentially the same as that for the collection efficiency or the kernel is not surprising because both the kernel and the ice size distribution functions are gamma-type functions. Even after they are multiplied and integrated, the resulting functions should still resemble the gamma-type function, as is the case here.

6. EXPERIMENTAL VERIFICATION OF THEORETICAL RESULTS

Experimental verification of the above theory is difficult to obtain. However, a recent field study by Sauter and Wang (1989) has yielded collection efficiency values of columns and needles for a 0.75-μm AP at 1013 mb and 273 K, with 85% r.h. These results are shown in Fig. 9 along with theoretical solutions for the same atmospheric conditions. Although the complicated shapes and irregularities of ice crystals prevent an exact comparison (e.g. the needles have irregularities and are not exactly columnar), the predictions of the theory are in good general agreement with this experiment.

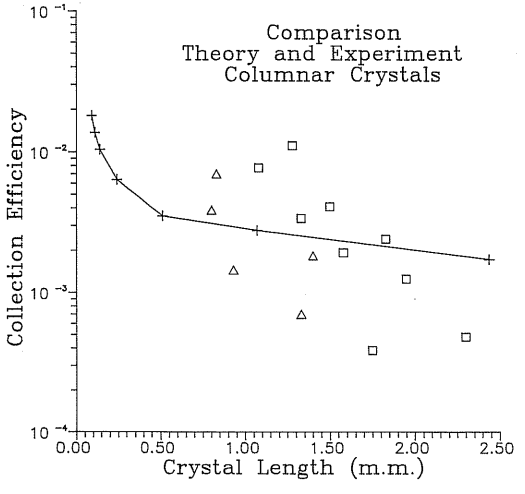

Fig. 9. Comparison of theoretical and experimental results of collection efficiency for aerosol particles by columnar ice crystals: ——, theory; Δ, needle (exp); □, column (exp).

7. CONCLUSIONS

A theoretical investigation of the collection of aerosol particles by columnar ice crystals and planar ice crystals has been presented. The results show that relative humidity, temperature, pressure, and electrostatic charge variations can alter the collection efficiency and rate across the Greenfield gap. This study quantitatively indicates that collection rates increase with decreasing relative humidity and increasing temperature, pressure, and electrostatic charge. The presence of a zero collection zone for planar ice crystals and columnar ice crystals agrees with observations of Wang *et al.* (1978) and Grover *et al.* (1977) for drops and with Martin *et al.* (1980a, b) for planar ice crystals. The zero collection zone is currently understood as a cancellation of radially directed forces when an aerosol particle is near a collector. This theoretical gap increases with increasing pressure or with decreasing temperature.

Acknowledgement—This work was supported by the U.S. Department of Energy, Assistant Secretary for Energy Research, Office of Health and Environmental Research, under contract W-31-109-ENG-38 and National Science Foundation grant ATM-9002299.

REFERENCES

Beard K. V. and Grover S. N. (1974) Numerical collision efficiencies for small raindrops colliding with microsize particles. *J. atmos. Sci.* **31,** 543–550.

Brock J. R. (1962) On the theory of thermal forces acting on aerosol particles. *J. Colloid Interf. Sci.* **17,** 768–780.

Carnuth W. (1967) Zur Abhaengigheit das Aerosol Partikel Spektrum von meteorogischen Vorgaengen und Zustaende. *Arch. Meteor. Geophys. Bioklim.* **16A,** 321–343.

Graedal T. E. and Franey J. P. (1975) Field measurements of submicron particle washout by snow. *Geophys. Res. Lett.* **2,** 325.

Greenfield S. (1957) Rain scavenging of radioactive particulate matter from the atmosphere. *J. Met.* **14,** 115–125.

Grover S. N. (1980) A numerical determination of the efficiency with which aerosol particles collide with cloud and small rain drops. Ph.D. thesis, University of California, Los Angeles.

Grover S. N., Pruppacher H. R. and Hamielec A. E. (1977) A numerical determination of the efficiency with which spherical aerosol particles collide with spherical water drops due to inertial impaction, phoretic, and electric forces. *J. atmos. Sci.* **36,** 1665–1669.

Hall W. D. and Pruppacher H. R. (1976) The survival of ice particles falling from cirrus clouds in subsaturated air. *J. atmos. Sci.* **33,** 1995–2006.

Hidy G. M. and Brock J. R. (1970) The dynamics of aerocolloidal systems. In *International Reviews in Aerosol Physics and Chemistry*, Vol. 1. Pergamon Press, Oxford.

Hobbs P. V., Radke L. F., Atkinson J. D., Robertson C. E., Weiss R. R., Turner F. M. and Brown R. R. (1972) Research Report VII, December 1972, Department of Atmospheric Science, University of Washington–Seattle.

Lai K. N., Dayan N. and Kerker M. (1978) Scavenging of aerosol particles by falling water drops. *J. atmos. Sci.* **35,** 674–682.

Leong K. H., Beard K. V. and Ochs H. (1982) Laboratory measurements of particle capture by evaporating cloud drops. *J. atmos. Sci.* **39,** 1130–1140.

Magono C., Endoh T., Harimayn T. and Kubota S. (1974) A measurement of scavenging effect of falling snow crystals on the aerosol concentration. *J. met. Soc. Japan* **52,** 407–416.

Magono C., Endoh T. and Itasaka M. (1975) Observation of aerosol particles attached to falling snow crystals. *J. Fac. Sci. Hokkaido Univ.* **4,** 103–119.

Martin J. J., Wang P. K. and Pruppacher H. R. (1980a) A theoretical study of the effect of elective charges on the efficiency with which aerosol particles are collected by ice crystal plates. *J. Colloid. Interf. Sci.* **78,** 44–55.

Martin J. J., Wang P. K. and Pruppacher H. R. (1980b) A theoretical determination of the efficiency with which aerosol particles are collected by simple ice crystal plates. *J. atmos. Sci.* **37,** 1628–1638.

Mason B. J. (1971) *The Physics of Clouds.* Oxford University Press.

Miller N. L. (1987) A theoretical investigation of the removal of aerosol particles by falling ice crystals. Doctoral thesis. University of Wisconsin, Madison, WI.

Miller N. L. (1990) A model for the determination of the scavenging rates of submicron aerosols by snow crystals. *Atmos. Res.* **25,** 317–330.

Miller N. L. and Wang P. K. (1989) Theoretical determination of the efficiency of aerosol particle collection by falling columnar ice crystals. *J. atmos. Sci.* **46,** 1656–1663.

Pilat M. J. and Prem A. (1976) Calculated particle collection efficiencies of single droplets including inertial impaction: brownian diffusion, diffusiophoresis and thermophoresis. *Atmospheric Environment* **10,** 13–19.

Pilat M. J. and Prem A. (1977) Effect of diffusion and thermophoresis on the overall particle collection efficiency of spray shop scrubbers. *J. Air Pollut. Control. Ass.* **27,** 982–988.

Pruppacher H. R. and Klett J. D. (1978) *Microphysics of Clouds and Precipitation.* D. Reidel, Dordrecht.

Sauter D. O. and Wang P. K. (1989) An experimental study of the scavenging of aerosol particles by natural snow crystals. *J. atmos. Sci.* **46,** 1600–1655.

Slinn W. G. N. and Hales J. M. (1970) Phoretic processes in scavenging. *Precipitation Scavenging,* AEC Symp. Ser, Richland, pp. 411–421.

Slinn W. G. N. and Hales J. M. (1971) A re-evaluation of the role of thermophoresis as a mechanism of in and below cloud scavenging. *J. atmos. Sci.* **28,** 1465–1471.

Wang P. K. (1983) Collection of aerosol particles by conducting sphere in an extended electric field-continue regime approximation. *J. Colloid Interf. Sci.* **94,** 301–318.

Wang P. K. (1985) A convective diffusion model for the scavenging of submicron aerosol particles by snow crystals of arbitrary shapes. *J. Rech. Atmos.* **19,** 185–191.

Wang P. K. (1989) A convective diffusion model for the scavenging of submicron aerosol particles by snow crystals of arbitrary shapes: some comments and corrections. *Atmos. Res.* **23,** 195–198.

Wang P. K. and Pruppacher H. R. (1977) An experimental determination of the efficiency with which aerosol particles are collected by water drops in subsaturated air. *J. atmos. Sci.* **34,** 1664–1669.

Wang P. K. and Pruppacher H. R. (1980a) On the efficiency with which aerosol particles of radius less than 1 μm are collected by columnar ice crystals. *Pure Applic. Geophys.* **118,** 1090–1108.

Wang P. K. and Pruppacher H. R. (1980b) The effect of an external electric field on the scavenging of aerosol particles by cloud and small raindrops. *J. Colloid Interf. Sci.* **75,** 286–297.

Wang P. K., Grover S. N. and Pruppacher H. R. (1978) On the effect of electric charges on the scavenging of aerosol particles by cloud and small rain drops. *J. atmos. Sci.* **35,** 1735–1743.